J|A|C|S
ARTICLES

Published on Web 04/10/2008

Origin of the Dendritic Effect in Multivalent Enzyme-Like Catalysts

Giovanni Zaupa, Paolo Scrimin,* and Leonard J. Prins*

Department of Chemical Sciences, University of Padova, and ITM-CNR Padova section, Via Marzolo 1, 35131 Padova, Italy

Received December 21, 2007; E-mail: leonard.prins@unipd.it; paolo.scrimin@unipd.it

Abstract: Functionalization of multivalent structures such as dendrimers and monolayer passivated nanoparticles with catalytically active groups results in very potent catalysts, a phenomenon described as the positive dendritic effect. Here, we describe a series of peptide dendrons and dendrimers of increasing generation functionalized at the periphery with triazacyclononane, a ligand able to form a strong complex with Zn^{II}. Kinetic studies show that these metallodendrimers very efficiently catalyze the cleavage of the RNA model compound HPNPP, with dendrimer D_{32} exhibiting a rate acceleration of around 80 000 (k_{cat}/k_{uncat}) operating at a concentration of 600 nM. A theoretical model was developed to explain the positive dendritic effect displayed by multivalent catalysts in general. A detailed analysis of the saturation profile and the Michaelis–Menten parameters k_{cat} and K_M shows that it is not necessary to ascribe the positive dendritic effect to, for instance, changes in the catalytic site, increased substrate binding constant, or changes in the microenvironment. Rather it appears that the efficient catalytic behavior of multivalent catalysts is mainly determined by two factors: the number of catalytic sites occupied by substrate molecules under saturation conditions, and the efficiency of the multivalent system to generate catalytic sites in which multiple catalytic units act cooperatively on the substrate.

1. Introduction

Multivalency is becoming a key concept in the fields of (bio)recognition,[1–4] catalysis,[5,6] supramolecular chemistry,[7] and nanotechnology.[8,9] The interest in multivalent structures, i.e., structures able to develop multiple single interactions with a target, originates from the awareness that multivalent interactions play a fundamental role in numerous biological processes.[10,11] The functionalization of multivalent molecular architectures, such as small tripodal scaffolds,[12] dendrimers,[13] polymers,[14] and surfaces,[15] with recognition and sensing elements, catalytic units, or markers is now rapidly leading toward new applications. In addition, theoretical studies start to unravel the fundamental aspects of multivalent interactions, and parameters are being developed to describe them.[16–18]

Our main interest is in developing multivalent enzyme-like catalysts, in which multivalent scaffolds are used to rapidly create multiple catalytic sites in which different functional groups can act in a cooperative manner on a substrate. So far, our attention has been devoted mainly to tripodal scaffold

(1) Handl, H. L.; Vagner, J.; Han, H.; Mash, E.; Hruby, V. J.; Gillies, R. J. *Exp. Opin. Ther. Targets* **2004**, *8*, 565–586.
(2) Kiessling, L. L.; Gestwicki, J. E.; Strong, L. E. *Angew. Chem., Int. Ed.* **2006**, *45*, 2348–2368.
(3) Lundquist, J. J.; Toone, E. J. *Chem. Rev.* **2002**, *102*, 555–578.
(4) Kiessling, L. L.; Gestwicki, J. E.; Strong, L. E. *Curr. Opin. Chem. Biol.* **2000**, *4*, 696–703.
(5) Dahan, A.; Portnoy, M. *J. Polym. Sci. Part A: Polym. Chem.* **2005**, *43*, 235–262.
(6) Breslow, R.; Belvedere, S.; Gershell, L.; Leung, D. *Pure Appl. Chem.* **2000**, *72*, 333–342.
(7) Badjiæ, J.; Nelson, A.; Cantrill, S. J.; Turnbull, W. B.; Stoddart, J. F. *Acc. Chem. Res.* **2005**, *38*, 723–732.
(8) Mulder, A.; Huskens, J.; Reinhoudt, D. N. *Org. Biomol. Chem.* **2004**, *2*, 3409–3424.
(9) Ludden, M. J. W.; Reinhoudt, D. N.; Huskens, J. *Chem. Soc. Rev.* **2006**, *35*, 1122–1134.
(10) Mammen, M.; Choi, S.-K.; Whitesides, G. M. *Angew. Chem., Int. Ed.* **1998**, *37*, 2754–2794.
(11) Varki, A. *Glycobiology* **1993**, *3*, 97–130.
(12) (a) For illustrative examples, see: Badjic, J. D.; Balzani, V.; Credi, A.; Silvi, S.; Stoddart, J. F. *Science* **2004**, *303*, 1845–1849. (b) Rao, J.; Lahiri, J.; Isaacs, L.; Weis, R. M.; Whitesides, G. M. *Science* **1998**, *280*, 708–711. (c) Kitov, P. I.; Sadowska, J. M.; Mulvey, G.; Armstrong, G. D.; Ling, H.; Pannu, N. S.; Read, R. J.; Bundle, D. R. *Nature* **2000**, *403*, 669–672.
(13) (a) For illustrative examples, see: Prinzen, L.; Miserus, R. J. H. M.; Dirksen, A.; Hackeng, T. M.; Decker, N.; Bitsch, N. J.; Megens, R. T. A.; Douma, K.; Heemskerk, J. W.; Kooi, M. E.; Frederik, P. M.; Slaaf, D. W.; Van Zandvoort, M. A. M. J.; Reutelingsperger, C. P. M. *Nano Lett.* **2007**, *7*, 93–100. (b) Kostiainen, M. A.; Szilvay, G. R.; Smith, D. K.; Linder, M. B.; Ikkala, O. *Angew. Chem., Int. Ed.* **2006**, *45*, 3538–3542. (c) Rameshwer, R.; Thomas, T. P.; Peters, J.; Kotlyar, A.; Myc, A.; Baker, J. R. J., Jr. *Chem. Commun.* **2005**, *573*, 9–5741. (d) Chang, T.; Rozkiewicz, D. I.; Ravoo, B. J.; Meijer, E. W.; Reinhoudt, D. N. *Nano Lett* **2007**, *7*, 978–980.
(14) (a) For illustrative examples, see: Renner, C.; Piehler, J.; Schrader, T. *J. Am. Chem. Soc.* **2006**, *128*, 620–628. (b) Haag, R.; Kratz, F. *Angew. Chem., Int. Ed.* **2006**, *45*, 1198–1215.
(15) (a) For illustrative examples, see: Dietrich, C.; Schmitt, L.; Tampé, R. *Proc. Natl. Acad. Sci. U.S.A.* **1995**, *92*, 9014–9018. (b) De Jong, M. R.; Huskens, J.; Reinhoudt, D. N. *Chem.—Eur. J.* **2001**, *7*, 4164–4170. (c) Thibault, R. J., Jr.; Galow, T. H.; Turnberg, E. J.; Gray, M.; Hotchkiss, P. J.; Rotello, V. M. *J. Am. Chem. Soc.* **2002**, *124*, 15249–15254.
(16) Huskens, J.; Mulder, A.; Auletta, T.; Nijhuis, C. A.; Ludden, M. J. W.; Reinhoudt, D. N. *J. Am. Chem. Soc.* **2004**, *126*, 6784–6797.
(17) Ercolani, G. *J. Am. Chem. Soc.* **2003**, *125*, 16097–16103.
(18) Kitov, P. I.; Bundle, D. R. *J. Am. Chem. Soc.* **2003**, *125*, 16271–16284.
(19) Scarso, A.; Scheffer, U.; Göbel, M.; Broxterman, Q. B.; Kaptein, B.; Formaggio, F.; Toniolo, C.; Scrimin, P. *Proc. Natl. Acad. Sci. U.S.A.* **2002**, *99*, 5144–5149.

molecules[19–21] and self-assembled monolayers on Au nanoparticles,[22–25] but recently we have also started to exploit dendrimers as multivalent scaffolds.[26] Dendrimers are monodispersed, hyperbranched polymers which have the advantage over nanoparticles and polymers that they are molecularly defined, which facilitates analysis.[27–30] Dendrimers have been extensively used in catalysis taking advantage of various dendrimer properties such as an ease of separation from the reaction mixture, the ability to create a specific microenvironment, or the induction of steric effects.[5,31–34] The similarity in size and molecular weight of dendrimers and proteins has led toward the development of dendrimers as artificial enzymes.[35–37] In seminal contributions, Reymond et al. showed that the screening of combinatorial libraries of peptide dendrimers can lead toward very potent catalysts displaying enzyme-like behavior.[38,39] It has been often observed that the potency of dendrimer catalysts dramatically increases with their valency, which is commonly referred to as a positive dendritic effect and ascribed to various chemical causes such as an altered pK_a of the active unit, changes in polarity, or increased substrate binding.[28,40–45] Here, we observe a similar positive dendritic effect in metallodendrimers of various generations which are very active in the catalytic cleavage of HPNPP, a model compound for RNA. Based on a theoretical model, we propose that the dendritic effect in this kind of multivalent system is related to the number of substrate molecules bound at saturation and the efficiency of the dendrimers in generating catalytic sites composed of two individual triazacyclononane−Zn^{II} complexes.

Previously, we have shown that a DAB (poly(propylene imine)) dendrimer functionalized at the periphery with 16 triazacyclononane (TACN) macrocycles in the presence of Zn^{II} very efficiently catalyzes the cleavage of 2-hydroxypropyl-*p*-nitrophenyl phosphate (HPNPP), which is the standard model of an RNA-phosphodiester.[26] Very importantly, by studying the catalytic activity of third generation dendrimers with different mole fractions of TACN-ligands at the periphery we were able to demonstrate that the catalytic activity results from the simultaneous action of two Zn^{II} metal ions on the substrate. In other words, dendrimer functionalization results in the formation of catalytic sites composed of two TACN−Zn^{II} complexes. We were interested to find out to which extent the formation of such catalytic sites depended on the dendrimer generation and set out to prepare a series of dendrimers of increasing generation fully covered at the periphery with TACN-ligands.

2. Results and Discussion

2.1. Synthesis of Dendrons d_2−d_{16} and Dendrimers D_4−D_{32}. Solution-phase functionalization of DAB dendrimers is rather cumbersome, especially for the higher generations, because of difficulties in driving reactions to completion and in product purification. To avoid these problems we decided to switch to the use of the very frequently used MAP dendrimers, which have a branched backbone composed of Lys residues (Chart 1).[46,47] These dendrimers can be readily synthesized and functionalized on a solid support using conventional peptide chemistry. Formally in terms of dendrimer terminology, cleavage from resin gives dendrons with a functional group at the focal point. In analogy with systems reported by Reymond et al. we decided to start the peptide synthesis with a small spacer (GlyCys) at the focal point for the following reasons (Scheme 1).[37,48] A small spacer separates the growing dendrimer backbone (Lys residues) from the resin which facilitates dendrimer growth. The Cys residue is of importance, first, because it allows dimerization of two dendrons to give a dendrimer via disulfide formation (Chart 1c) and, second, because the thiol residue can be used to quantify unambiguously the concentration of dendron in a solution using Ellman's reagent.

The synthesis of dendrons d_2−d_8 was performed on Rink AM resin with an initial loading of 0.65 mmol/g. The largest dendron d_{16} was synthesized on Tentagel RAM with a reduced loading of 0.35 mmol/g, because the addition of the last Lys generation could not be driven to completion on the original resin. Quantitative coupling of each new Lys generation was in all cases confirmed by a negative Kaiser test and a doubling of the amount of dibenzofulvene−piperidine adduct liberated upon Fmoc deprotection. The TACN macrocycle was introduced as reported before using an acetate functionalized with diBOC-protected triazacyclononane.[26] Cleavage from resin yielded dendrons d_2−d_{16} which were purified by RP HPLC and characterized by MALDI-TOF or ESI-MS analysis. Stock solutions of the respective dendrons were prepared in a 1:1 mixture of H_2O/CH_3CN, the concentration of which was determined using Ellman's reagent. Before using these dendrons in catalysis, the thiol unit was deactivated via reaction with 1

(20) Scarso, A.; Zaupa, G.; Bodar Houillon, F.; Prins, L. J.; Scrimin, P. *J. Org. Chem.* **2007**, *72*, 376–385.
(21) Zaupa, G.; Martin, M.; Prins, L. J.; Scrimin, P. *New J. Chem.* **2006**, *30*, 1493–1497.
(22) Pasquato, L.; Pengo, P.; Scrimin, P. *J. Mater. Chem.* **2004**, *14*, 3481–3487.
(23) Pengo, P.; Baltzer, L.; Pasquato, L.; Scrimin, P. *Angew. Chem., Int. Ed.* **2007**, *46*, 400–404.
(24) Manea, F.; Bodar-Houillon, F.; Pasquato, L.; Scrimin, P. *Angew. Chem., Int. Ed.* **2004**, *43*, 6165–6169.
(25) Pengo, P.; Polizzi, S.; Pasquato, L.; Scrimin, P. *J. Am. Chem. Soc.* **2005**, *127*, 1616–1617.
(26) Martin, M.; Manea, F.; Fiammengo, R.; Prins, L. J.; Pasquato, L.; Scrimin, P. *J. Am. Chem. Soc.* **2007**, *129*, 6982–6983.
(27) Tomalia, D. A.; Naylor, A. M.; Goddard, W. A. *Angew. Chem., Int. Ed. Engl.* **1990**, *29*, 138–175.
(28) Fréchet, J. M. J. *Science* **1994**, *263*, 1710–1715.
(29) Grayson, S. M.; Fréchet, J. M. J. *Chem. Rev.* **2001**, *101*, 3819–3867.
(30) Bosman, A. W.; Janssen, H. M.; Meijer, E. W. *Chem. Rev.* **1999**, *99*, 1665–1688.
(31) Chow, H.-F.; Leung, C.-F.; Wang, G.-X.; Yang, Y.-Y. *C. R. Chimie* **2003**, *6*, 735–745.
(32) Helms, B.; Fréchet, J. M. J. *Adv. Synth. Catal.* **2006**, *348*, 1125–1148.
(33) Twyman, L. J.; King, A. S. H.; Martin, I. K. *Chem. Soc. Rev.* **2002**, *31*, 69–82.
(34) Hecht, S.; Fréchet, J. M. J. *Angew. Chem., Int. Ed.* **2001**, *40*, 74–91.
(35) Liang, C.; Fréchet, J. M. J. *Prog. Polym. Sci.* **2005**, *30*, 385–402.
(36) Darbre, T.; Reymond, J.-L. *Acc. Chem. Res.* **2006**, *39*, 925–934.
(37) Esposito, A.; Delort, E.; Lagnoux, D.; Djojo, F.; Reymond, J.-L. *Angew. Chem., Int. Ed.* **2003**, *42*, 1381–1383.
(38) Clouet, A.; Darbre, T.; Reymond, J.-L. *Angew. Chem., Int. Ed.* **2004**, *43*, 4612–4615.
(39) Javor, S.; Delort, E.; Darbre, T.; Reymond, J. L. *J. Am. Chem. Soc.* **2007**, *129*, 13238–13247.
(40) Delort, E.; Darbre, T.; Reymond, J.-L. *J. Am. Chem. Soc.* **2004**, *126*, 15642–15643.
(41) Dahan, A.; Portnoy, M. *Org. Lett.* **2003**, *5*, 1197–1200.
(42) Ribourdouille, Y.; Engel, G. D.; Richard-Plouet, M.; Gade, L. H. *Chem. Commun.* **2003**, 1228–1229.
(43) Ropartz, L.; Morris, R. E.; Foster, D. F.; Cole-Hamilton, D. J. *Chem.Commun.* **2001**, 361–362.
(44) Kleij, A. V.; Gossage, R. A.; Jastrzebski, J.T.B.H.; Boersa, J.; Van Koten, G. *Angew. Chem., Int. Ed.* **2000**, *39*, 176–178.
(45) Breinbauer, R.; Jacobsen, E. N. *Angew. Chem., Int. Ed.* **2000**, *39*, 3604–3607.
(46) Sadler, K.; Tam, J. P. *Rev. Mol. Biotechnol.* **2002**, *90*, 195–229.
(47) Crespo, L.; Sanclimens, G.; Pons, M.; Giralt, E.; Royo, M.; Albericio, F. *Chem. Rev.* **2005**, *105*, 1663–1681.
(48) Lagnoux, D.; Delort, E.; Douat-Casassus, C.; Esposito, A.; Reymond, J.-L. *Chem.−Eur. J.* **2004**, *10*, 1215–1226.

Chart 1[a]

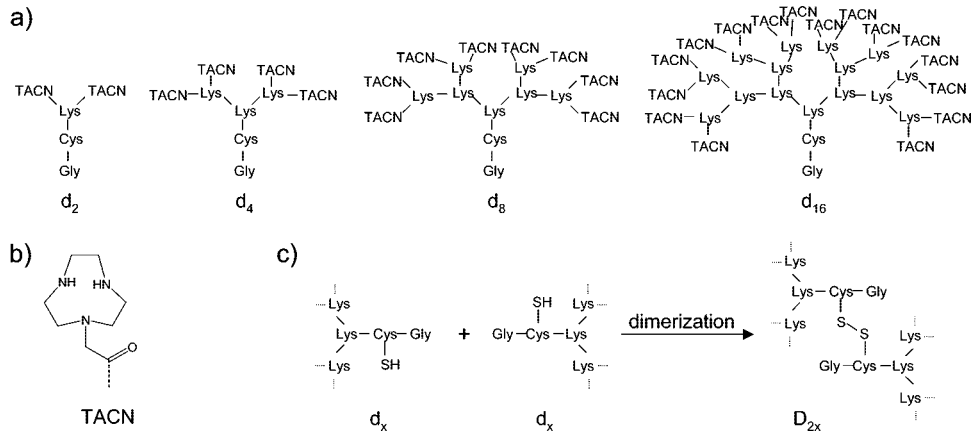

[a] (a) Dendrons d_2-d_{16}, (b) the ligand triazacyclononane TACN, and (c) formation of dendrimers D_4-D_{32} by dimerization of the respective dendrons.

Scheme 1. Synthesis of TACN-Functionalized Dendrons on Solid Support

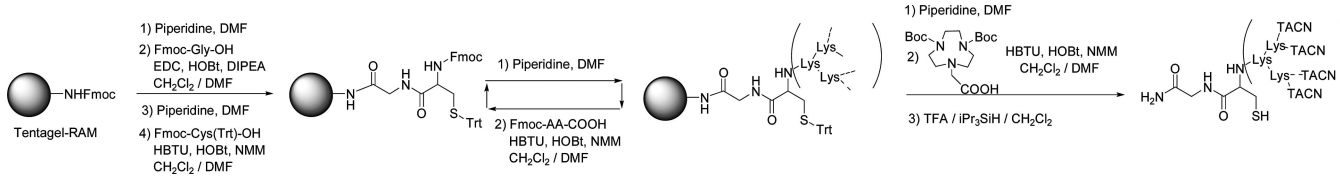

equiv of *N*-ethylmaleimide. The quantitative reaction was confirmed by a negative Ellman's test. Dimerization of dendrons to give dendrimers D_4-D_{32} was performed by bubbling air through a solution of the dendron in a 1:1 mixture of H_2O basified at pH 10 with NaOH and CH_3CN. Also in this case, quantitative dimerization was confirmed by a complete absence of any signal indicating free thiol using Ellman's reagent and the presence of a single new peak in the HPLC spectrum.

2.2. Catalytic Cleavage of HPNPP. In analogy with our previous studies,[26] it was decided that the catalytic activity of all dendrons d_2-d_{16} and dendrimers D_4-D_{32} was to be studied at *a constant concentration of TACN* rather than at a constant dendrimer concentration. Thus, any changes in catalytic activity can be directly related to the valency of the dendrimer. Consequently, at a constant TACN concentration of 20 μM this implies that dendrimer D_{32} is present at a 600 nM concentration. First, the catalytic activity of all multivalent catalysts in the cleavage of HPNPP (Figure 1a) was studied in the presence of increasing amounts of Zn^{II} in a 7:3 H_2O/CH_3CN mixture buffered at pH 7.5 at 40 °C. Plots of the initial rate as a function of the number of equivalents of Zn^{II} (per TACN) in all cases clearly show a sigmoidal increase in activity up to 1 equiv of Zn^{II}, after which the catalytic activity remains constant (Figure 1b,c). This behavior is identical to that observed previously with the DAB dendrimers[26] and confirms that also here the 1:1 complex TACN$-Zn^{II}$ is the catalytically active unit. The fact that all curves level off at constant values also indicates that the contribution of free Zn^{II} to catalysis can be neglected.

Importantly, although performed at a constant concentration of TACN, the Zn^{II} titration studies also clearly indicate an increase in catalytic activity upon an increase of the dendron and dendrimer valency. The catalytic performance of these systems was studied in detail by measuring the initial rates in the presence of increasing amounts of substrate HPNPP, i.e., under turnover conditions, in the presence of 1 equiv of Zn^{II} per TACN unit (Figure 2). All catalysts display enzyme-like saturation behavior with multiple turnovers, and the Michaelis–Menten parameters k_{cat} and K_M were determined for each catalyst by fitting the saturation curves to the Michaelis–Menten equation $v_{init} = k_{cat}[E][S]/(K_M + [S])$. It should be emphasized that the

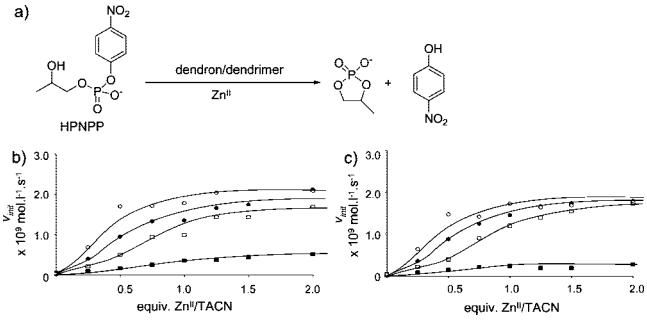

Figure 1. Initial rates for (a) the cleavage of HPNPP by (b) dendrons d_2 (■), d_4 (□), d_6 (●), and d_8 (○) and (c) dendrimers D_4 (■), D_8 (□), D_{16} (●), and D_{32} (○), as a function of the equivalents of Zn^{II} added with respect to [TACN]. The solid lines are trendlines. Conditions: [TACN] = 2×10^{-5} M, [HPNPP] = 2×10^{-4} M, [HEPES] = 1×10^{-2} M, pH = 7.5, T = 40 °C, H_2O/CH_3CN = 7:3.

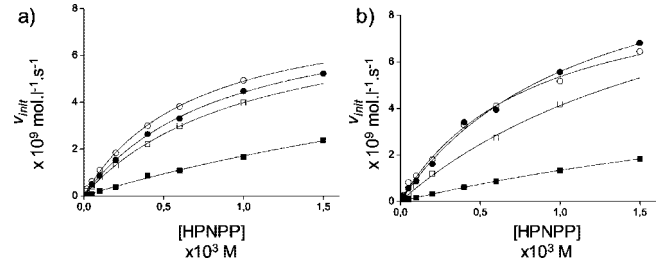

Figure 2. Initial rates for the cleavage of HPNPP by (a) dendrons d_2 (■), d_4 (□), d_6 (●), and d_8 (○) and (b) dendrimers D_4 (■), D_8 (□), D_{16} (●), and D_{32} (○), as a function of substrate concentration. Conditions: [TACN] = 2×10^{-5} M, [Zn^{II}] = 2×10^{-5} M, [HEPES] = 1×10^{-2} M, pH = 7.5, T = 40 °C, H_2O/CH_3CN = 7:3. Solid lines indicate the best fits to the Michaelis–Menten equation.

Table 1. Michaelis–Menten Parameters for Dendrons d_2–d_{16} and Dendrimers D_4–D_{32}[a]

	no. TACN	$k_{cat,den}$ ($\times 10^3$ s^{-1})	$k_{cat,unit}$ ($\times 10^4$ s^{-1})	K_M ($\times 10^3$ M)	$k_{cat,den}/K_M$ ($L \cdot mol^{-1} \cdot s^{-1}$)	$k_{cat,den}/k_{uncat}$[b]
d_2	2	0.6	3.2	2.8	0.2	3190
D_4	4	1.3	3.4	4.0	0.3	6710
d_4	4	1.6	4.1	1.0	1.6	8120
D_8	8	4.8	6.0	1.9	2.5	24000
d_8	8	3.3	4.1	0.9	3.8	16600
D_{16}	16	9.6	6.0	1.2	8.4	48000
d_{16}	16	6.7	4.2	0.7	9.5	33400
D_{32}	32	15.6	4.9	0.8	19.0	78200

[a] Conditions as given in the legend of Figure 2. [b] $k_{uncat} = 2 \times 10^{-7}$ s^{-1}.[26]

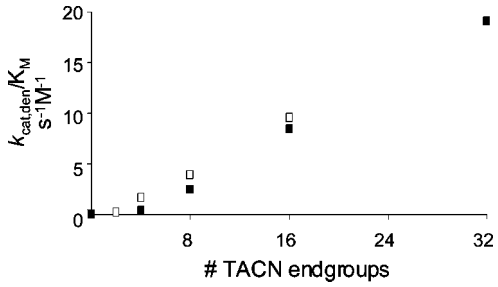

Figure 3. Dendritic effect of dendrons d_2–d_{16} (□) and dendrimers D_4–D_{32} (■) in the cleavage of HPNPP.

value of k_{cat} depends on what is considered the catalyst concentration [E]. Generally,[37,38,50] the dendron/dendrimer concentration is taken as a reference, which gives a $k_{cat,den}$ value describing the overall performance of the multivalent catalyst. Alternatively, by taking the concentration of TACN as reference, the $k_{cat,unit}$ value is the rate constant corrected for the number of ligands present in the multivalent catalyst ($k_{cat,den} = k_{cat,unit} \times$ no. of catalyst units). The difference between these parameters will be discussed extensively later. For the moment, in line with the general interpretation of multivalent catalysts of this type,[35–37,50] the overall parameter $k_{cat,den}$ will be used. Table 1 lists all parameters including the rate acceleration ($k_{cat,den}/k_{uncat}$) with respect to the uncatalyzed reaction ($k_{uncat} = 2 \times 10^{-7}$ s^{-1}).[26]

The obtained Michaelis–Menten parameters are clearly indicative of a strong dendritic effect. The data of Table 1 and the plot of Figure 3 indicate that the combination of a continuously increasing $k_{cat,den}$ and decreasing K_M values causes an exponential growth of the second-order rate constant $k_{cat,den}/K_M$ as a function of the catalyst valency. Dendrimer D_{32}, present in submicromolar concentrations, induces a rate enhancement of around 80 000 with respect to the uncatalyzed cleavage of HPNPP, which ranks it among the most potent catalysts reported so far.[49–52,24]

These data indicate that the clustering of multiple copies of a simple TACN-ligand on the surface of a multivalent dendrimer is enough to generate an extremely powerful catalyst. This "dendritic" effect appears very general, since we have observed similar behavior now for a wide variety of multivalent scaffolds, including small tripodal structures,[19,20] SAMs on Au nanoparticles,[24] and the DAB dendrimers[26] reported before. This general trend, also evidenced by related systems reported in the literature, raised two questions which will be addressed here: (a) what is the origin of the dendritic effect and (b) what is the significance of the reported Michaelis–Menten parameters for multivalent catalysts.

2.3. Theoretical Model and Simulations. Although a very common approach, the fitting of the saturation curves obtained for multivalent catalysts to the Michaelis–Menten equation is not correct. The Michaelis–Menten equation specifically describes the situation in which one substrate molecule, S, binds to the single catalytic site in an enzyme, E, with a dissociation constant K_M, after which it is transformed into product, P, with a first-order rate constant k_{cat}.[53] However, multivalent catalysts as studied by us and others are intrinsically different from enzymes in the sense that they contain a multitude of catalytic sites. Consequently, under saturation conditions multiple substrate molecules are bound to the catalyst resulting in a multicomponent complex ES_n (with n depending on the number of catalytic sites present). Fitting of the saturation curve of such a system using the Michaelis–Menten equation gives composite values for K_M and k_{cat}, which incorporate all the separate binding and catalytic events that occur. We were interested in finding the relation between these "averaged" parameters and the individual parameters of a catalytic site. For that purpose a theoretical model was developed taking into account all separate binding and catalytic events that occur in a multivalent catalyst. The model is schematically depicted in Figure 4.

The starting point is a multivalent catalyst E_n, in which n denotes the number of catalytic units. Catalysis occurs either by a single catalytic unit (*single site catalysis*) or by the simultaneous action of two catalytic units (*double site catalysis*), each of them characterized by different binding (K_{mo}, K_{di}) and rate (k_{mo}, k_{di}) constants. The maximum number of substrate molecules, S, bound to a multivalent catalyst, E_n, equals n in case the catalytic site is composed of a single catalytic unit. When the catalytic site is composed of two catalytic units, the maximum number of bound substrate molecules is equal to $n/2$ or $(n - 1)/2$ in case n is an odd number. In the model, statistical coefficients (see Supporting Information) affect the association constants between binding site and substrate, and therefore the equilibrium constants in this model define association, which is opposite to the Michaelis–Menten parameter, K_M, which is generally defined as a dissociation constant. It should be noted that this model bears a strong resemblance to a model recently used by Huskens and Reinhoudt et al. to describe the interaction of a multivalent guest with a multivalent monolayer of hosts.[16]

The model is based on the following assumptions/criteria:

• All binding events are noncooperative. In other words, binding of a substrate has no effect on the binding constant of the subsequent substrate molecule.

• The binding and rate constants for the catalytic sites composed of one (K_{mo}, k_{mo}) or two (K_{di}, k_{di}) units are constant and independent of the size of the multivalent catalyst.

• In this theoretical model statistical coefficients account for *all* the possible modes in which a specific complex between substrate and catalytic site can be formed. No cut-offs in terms

(49) (a) For reviews on artificial nucleases, see: Williams, N. H.; Takasaki, B.; Wall, M.; Chin, J. *Acc. Chem. Res.* **1999**, *32*, 485–493. (b) Morrow, J. R.; Iranzo, O. *Curr. Opin. Chem. Biol.* **2004**, *8*, 192–200. (c) Mancin, F.; Scrimin, P.; Tecilla, P.; Tonellato, U. *Chem. Commun.* **2005**, 2540–2548.

(50) Avenier, F.; Domingos, J. B.; Van Vliet, L.; Hollfelder, F. *J. Am. Chem. Soc.* **2007**, *129*, 7611–7619.

(51) Molenveld, P.; Stikvoort, W. M. G.; Kooijman, H.; Spek, A. L.; Engbersen, J. F. J.; Reinhoudt, D. N. *J. Org. Chem.* **1999**, *64*, 3896–3906.

(52) Feng, G.; Natale, D.; Prabaharan, R.; Mareque-Rivas, J. C.; Williams, N. H. *Angew. Chem., Int. Ed.* **2006**, *45*, 7056–7059.

(53) Kirby, A. J. *Angew. Chem., Int. Ed. Engl.* **1996**, *35*, 707–724.

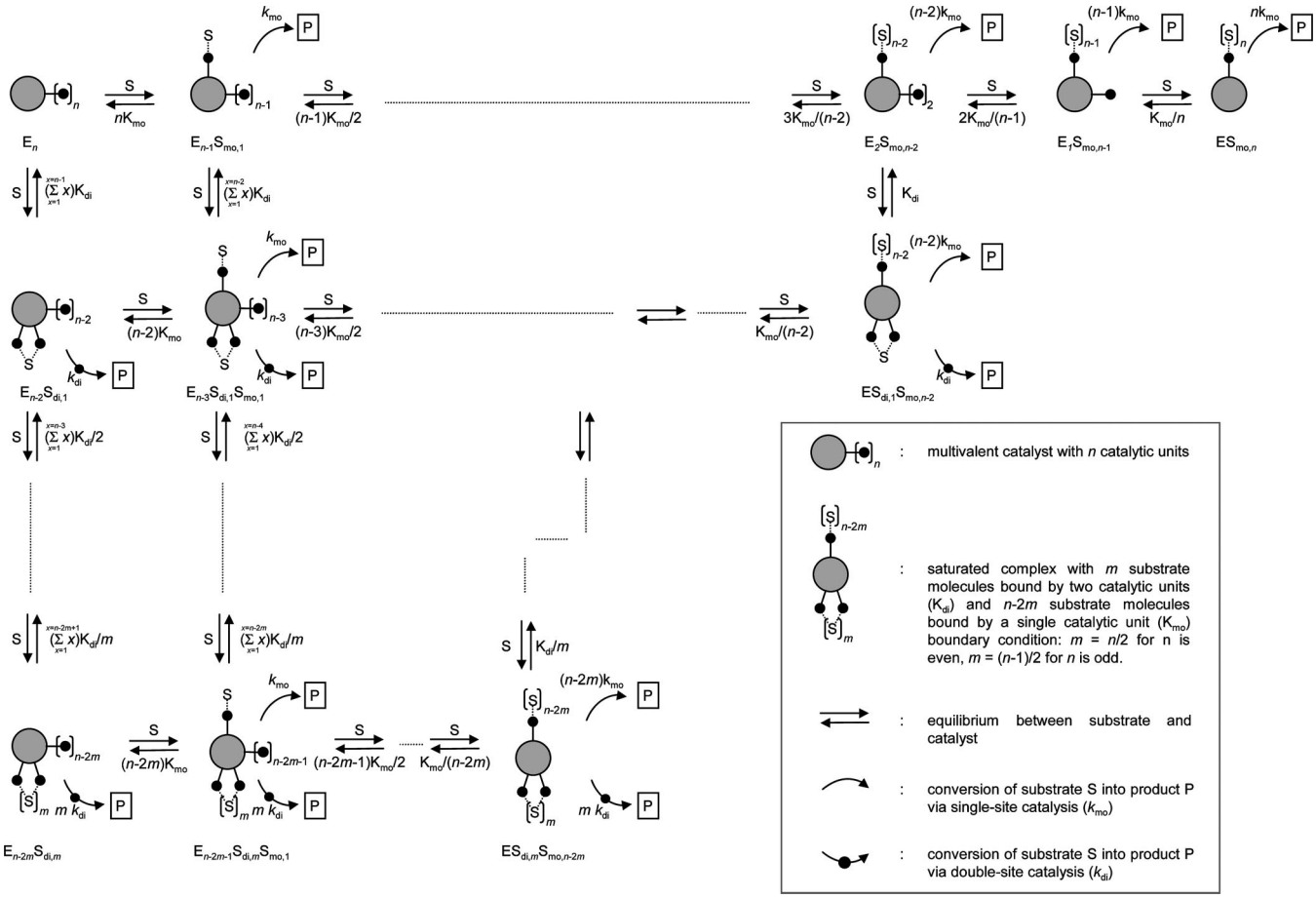

Figure 4. Theoretical model describing all separate binding and catalytic events that occur in a multivalent catalyst E_n. Within the multivalent catalyst binding and catalysis can occur via a single catalytic unit (K_{mo}, k_{mo}) or via the cooperative action of two catalytic units (K_{di}, k_{di}). In the model, the equilibrium constants K_{mo} and K_{di} are used as association constants.

of distance between catalytic units are present. The validity of this assumption will be discussed later.

Using this model the catalytic behavior of a series of multivalent catalysts E_2-E_8 with 2 up to 8 catalytic units (n = 2–8) was evaluated.[54] Values for association and rate constants were arbitrarily set to values that resemble our experimental data. We were interested in simulating the saturation curves for these multivalent catalysts under three different conditions, representing limiting cases:

• Catalysis only occurs via a single catalytic unit ($K_{mo} = 500$ M^{-1}, $k_{mo} = 1 \times 10^{-4}$ s^{-1}). Catalytic sites composed of two units are not considered. In the model (Figure 4) this implies that only the first row is taken into consideration.

• Catalysis occurs either by a single catalytic unit (K_{mo} = 500 M^{-1}, $k_{mo} = 1 \times 10^{-4}$ s^{-1}) or by the simultaneous action of two catalytic units ($K_{di} = 750$ M^{-1}, $k_{di} = 1 \times 10^{-3}$ s^{-1}). The catalytic site composed of two units is characterized by stronger binding and a higher rate constant.

• The catalytic activity of the multivalent catalyst originates only from double site catalysis ($K_{di} = 750$ M^{-1}, $k_{di} = 1 \times 10^{-3}$ s^{-1}), whereas the activity of the single catalytic units is ignored. In the model (Figure 4) this implies that only the first column is taken into consideration.

In accordance with our experimental data, all simulations were performed at a constant concentration of *catalytic units* (20 μM),

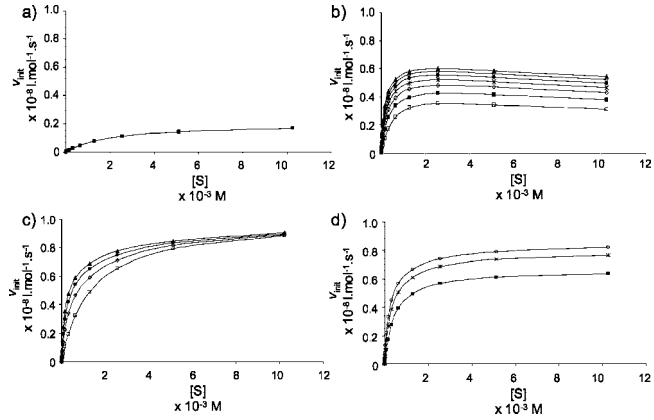

Figure 5. Calculated saturation behavior of multivalent catalyst models E_2-E_8 for situations in which catalysis results (a) only from single catalytic units (all models give an identical curve), (b) from both single and double site catalysis, and (c,d) from only double site catalysis in which the curves for the catalysts containing an even (c) or an odd (d) number of catalytic units are separated. The symbols denote E_2 (□), E_3 (■), E_4 (◊), E_5 (*), E_6 (●), E_7 (○), and E_8 (▲).

calculating for each multivalent catalyst E_2-E_8 the initial rate (v_{init}) as a function of the initial substrate concentration ($[S]_0$). The calculated saturation curves are shown in Figure 5a–d.

2.3.1. Single Site Catalysis ($K_{mo} = 500$ M^{-1}, $k_{mo} = 1 \times 10^{-4}$ s^{-1}). Under these conditions all multivalent catalysts E_2-E_8 have an identical saturation profile, which is identical to the saturation

(54) The models for E_2-E_8 were implemented in MicroMath Scientist for WindowsTM, version 2.01. For details, see the Supporting Information.

profile of the monomeric catalytic site (Figure 5a). The identical behavior of the models confirms the validity of the statistical coefficients used in the model.

2.3.2. Both Single and Double Site Catalysis ($K_{mo} = 500\ M^{-1}$, $k_{mo} = 1 \times 10^{-4}\ s^{-1}$, $K_{di} = 750\ M^{-1}$, $k_{di} = 1 \times 10^{-3}\ s^{-1}$). A different situation is observed in case also two catalytic units can simultaneously act on a substrate. Analyzing the simulated saturation curves, a first observation is that all curves go through a maximum after which the initial rate drops (Figure 5b). The reason is that initially the substrate binds to two catalytic units, ($K_{di} > K_{mo}$), and is transformed at a higher rate ($k_{di} > k_{mo}$). Subsequently, the substrate saturates the multivalent catalyst leading to a situation (which is not yet reached in the simulations) in which each catalytic unit has one substrate molecule bound (E_nS_n). A second observation is that the maximum value of v_{init} increases with the number of catalytic sites in the multivalent system with a concomitant steeper slope for low substrate concentrations.

2.3.3. Double Site Catalysis ($K_{di} = 750\ M^{-1}$, $k_{di} = 1 \times 10^{-3}\ s^{-1}$). For these conditions, multivalent models containing an even or odd number of catalytic units exhibit a different saturation behavior (Figures 5c and d, respectively). Models with an "even" number all saturate at the same v_{init}, but this maximum level is reached at lower substrate concentrations when the valency of the system increases. The "odd" models saturate at lower v_{init} values, which depend on the number of catalytic units present. As the valency increases the difference between the saturation of the "odd" and "even" models becomes smaller. As will be discussed later, the difference between "odd" and "even" models is of importance, since it gives an explanation for the experimentally observed difference between dendrons and dendrimers.

2.4. Analysis of the Simulations. The simulations clearly demonstrate that the saturation behavior of a multivalent catalyst strongly depends on its valency, *keeping constant* the Michaelis–Menten parameters for the individual catalytic sites and excluding any cooperative effect. This means that the observation of a change in saturation profile for dendrimer catalysts of different generations does not necessarily indicate an increased cooperativity or a higher catalytic efficiency. This will become more clear from the following analysis. We were curious as to what would happen if we used the calculated saturation curves (Figure 5) as "experimental" input for the classical Michaelis–Menten equation, since this is exactly how the saturation profiles of multivalent catalysts are commonly analyzed. This analysis was performed on the third set of simulations (only double site catalysis) for the simple reason that this situation bears the most resemblance to the experimental observations. The first simulation (only single site catalysis) is not interesting. Since only single catalytic units are involved, obviously there is no reason to gain any benefit from incorporating multiple units in a multivalent system. In the type of enzyme-like multivalent catalysts studied here, the dendritic effect originates from the fact that catalysis involves the simultaneous action of two catalytic units in the chemical transformation. The second simulation takes into account both single and double site catalysis, but in most experimental cases the catalytic activity of a single unit can be neglected with respect to double site catalysis ($k_{mo} << k_{di}$). Additionally, to the best of our knowledge, no example of a saturation profile for a multivalent catalyst in which v_{init} goes through a maximum has been reported. This indicates that generally the affinity of the substrate for the double sites is much higher than that for the single site

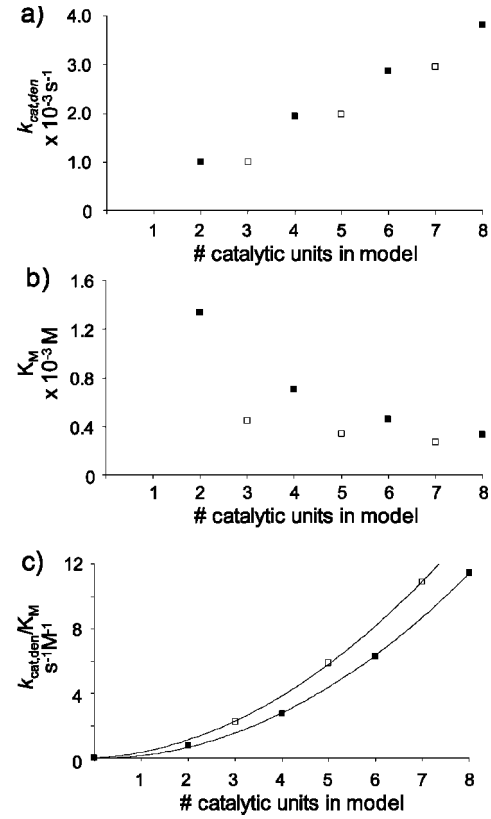

Figure 6. Michaelis–Menten parameters (a) $k_{cat,den}$, (b) K_M, and (c) $k_{cat,den}/K_M$ for models E_2-E_8 obtained by fitting the calculated saturation curves from Figure 5c and d (■: "even" models, □: "odd" models).

($K_{di} >> K_{mo}$).[55] The third simulation, therefore, bears the most relevance to the behavior of these multivalent catalysts.[56] Accordingly, the simulated saturation curves of Figure 5c and d were fitted using the Michaelis–Menten equation $v_{init} = (k_{cat,den}[E][S])/(K_M + [S])$. In order to stay in line with common enzyme terminology and enzyme model analysis, the Michaelis–Menten parameter K_M, describing dissociation, will be used from now on. Figure 6a–c give the Michaelis–Menten parameters that are generally used to describe the catalytic efficiency of multivalent catalyst, *i.e.*, $k_{cat,den}$, K_M, and the second-order rate constant $k_{cat,den}/K_M$. The results for the "odd" and "even" models are indicated separately. Both series display very similar trends for all parameters, but between them a very interesting difference exists. The analysis will be initially focused on the "even" models, bearing in mind that the discussion is valid also for the "odd" models.

The outcome of this "retro"-fitting gives very surprising results. As expected, the first-order rate constant $k_{cat,den}$ as a function of valency always increases accounting for the numerical increase of catalytic units present in the model. Remarkably, the "overall" dissociation constant K_M decreases

(55) A study of the saturation behavior of the single TACN–Zn^{II} complex under the same experimental conditions as those for the dendrimers give a strictly linear behavior between v_{init} and [HPNPP] (see Supporting Information), indicating indeed a very low binding constant between the single TACN–Zn^{II} complex and HPNPP. This supports our assumption to ignore single site catalysis.

(56) An additional analysis of Figure 5b, in which also single sites contribute to catalysis, leads to the same conclusions. This is described in detail in the Supporting Information. Summarizing, the presence of concomitant single and double site catalysis leads towards a less pronounced dendritic effect and a disappearance of the "odd/even" effect (see later).

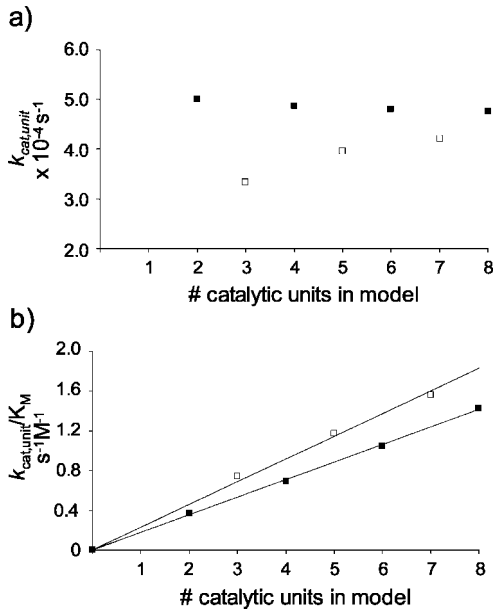

Figure 7. (a) First-order rate constant per catalytic unit ($k_{cat,unit} = k_{cat,den}/n$) and (b) the effect on $k_{cat,unit}/K_M$ for "even" (■) and "odd" (□) models.

in an asymptotic manner as a function of the valency, *suggesting* that substrate binding becomes stronger as the valency of the structure increases. As a result of these effects, the second-order rate constant $k_{cat,den}/K_M$ exponentially increases as a function of valency, which in the literature has been described as a *strong positive dendritic effect*.[32,40,41] It should be explicitly remembered, though, that the Michaelis–Menten parameters for the individual catalytic site *and* the concentration of catalytic units *were kept identical for all models* E_2-E_8. Apparently, the strong dendritic effect is a phenomenon that is *not necessarily related* to a change in either the catalytic (k_{di}) or binding constant (K_{di}) of the individual catalytic site. In order to discover the true origin of the dendritic effect the two parameters $k_{cat,den}$ and K_M will be discussed separately.

2.4.1. Catalytic Constant $k_{cat,den}$. The numerical increase of the number of catalytic units upon increasing valency automatically generates a higher value for $k_{cat,den}$ for each successive generation. In fact, corrected for the number of catalytic sites, a new constant $k_{cat,unit}$ ($k_{cat,den}/n$) can be defined which is now indeed constant for the "even" models (Figure 7a). Removing the numerical effect of $k_{cat,den}$ obviously also affects the second-order rate constant $k_{cat,unit}/K_M$ which now increases linearly with the valency (Figure 7b). However, albeit no longer exponential, the increase of $k_{cat,unit}/K_M$ is still an important dendritic effect, which is entirely due to changes in K_M.

2.4.2. Dissociation Constant K_M. The dendritic effect clearly originates from a decrease in the overall K_M upon an increase in valency, notwithstanding the fact that the K_M for a single catalytic site was kept constant. The reason for this particular behavior is exemplified for binding of substrate molecules to multivalent models E_2 and E_4. The clustering of 12 catalytic units in a divalent system (E_2) generates 6 catalytic sites (Figure 8, top left). However, clustering of the same number of catalytic units in a tetravalent system (E_4) generates 18 catalytic sites (Figure 8, top right). Increasing the valency of the system causes an exponential growth of the number of potential catalytic sites. This is visualized by plotting the number of available (double) binding sites for the first substrate molecule against valency (Figure 9, ■). As comparison, also the (linear) increase in single

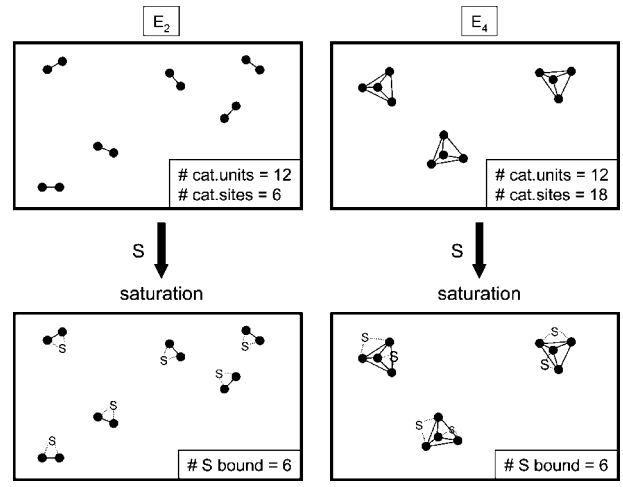

Figure 8. Effect of the clustering of catalytic units on the creation of catalytic sites in multivalent models E_2 and E_4. Each catalytic unit is depicted by a black circle (●), each catalytic site by a line connecting two catalytic units (−).

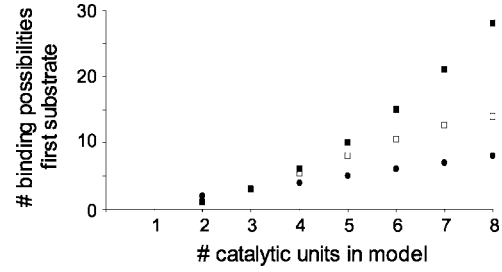

Figure 9. Number of potential catalytic sites for binding of the first substrate to models E_2-E_8 (●: single binding sites, ■: double binding sites, □: double binding sites corrected).

binding sites is depicted (Figure 9, ●). Obviously, similar statistical effects are also present for the binding of subsequent substrate molecules. Interestingly, however, at saturation both models E_2 and E_4 have an identical number of 6 substrate molecules bound (Figure 8, bottom), which explains that under these conditions no difference in catalytic activity is observed between them (since $k_{cat,unit}$ is constant). This analysis shows that the clustering of catalytic units in a multivalent system causes an increase in the "apparent" concentration of catalytic sites, resulting in an higher "apparent" substrate binding. It appears that this is the main origin for the dendritic effect.

The extent of the dendritic effect is determined by the number of catalytic sites that are formed upon clustering catalytic units in a multivalent system. As indicated before, in setting up the theoretical model it was assumed that in models E_2-E_8 all possible combinations of single catalytic units can form a double binding site. In practice, this may be true for catalysts with a low valency (3,4) but is rather unlikely for real multivalent systems in which spatial distances may prevent the cooperative action of two catalytic units on a substrate. In order to perform simulations that more closely resemble such an experimental situation, the statistical coefficients were altered. It was assumed that starting from dendrimer E_3 each subsequent generation loses 10% of the potential binding sites composed of two catalytic units for binding of the first (and also subsequent) substrate molecules. As an example, the new coefficients for binding of the first substrate are shown in Figure 9 (□). For dendrimer model E_8 the number of accessible binding sites for the first substrate is reduced by 50%. The number of possibilities to bind

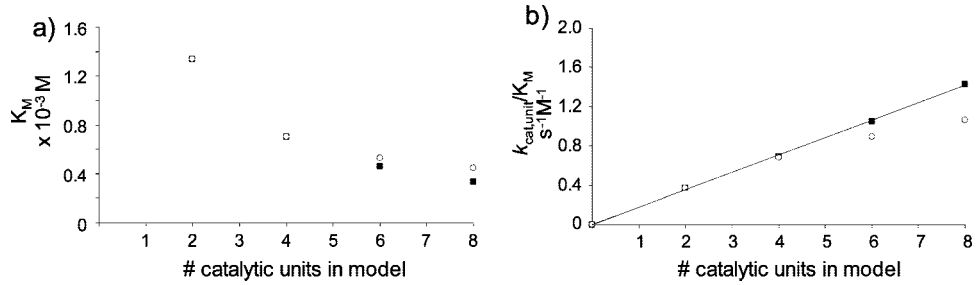

Figure 10. Effect of reduced statistical coefficients on (a) K_M and (b) $k_{cat,unit}/K_M$ for "even" dendrimers (■: maximized coefficients, ○: reduced coefficients).

four substrates (E_8S_4) is reduced by almost 70%. Using these new coefficients new saturation profiles were calculated (assuming only double site catalysis) and "retro"-fitted using the Michaelis–Menten equation. Obviously, the statistical coefficients do not affect the saturation level of each dendrimer, and consequently the newly obtained $k_{cat,unit}$ values are identical to those shown in Figure 7a. The changes in K_M and $k_{cat,unit}/K_M$ are given in Figure 10a and 10b together with those obtained from the first set of simulations. For reasons of clarity only those for the "even" models are shown (a same trend is observed for the "odd" models). For the models with high valency the effect of reducing the available binding sites results, as expected, in a less pronounced decrease in K_M and, as a consequence, a smaller increase in $k_{cat,unit}/K_M$. However, considering the fact that for E_8 up to 50% of the potential sites for the first substrate molecule has been removed, the effect on these parameters is surprisingly small. This is a clear indication that the observed phenomenon is not just a theoretical possibility but also a very plausible explanation for experimental observations. That this is indeed the case will be shown next, when our own experimental data are analyzed. However, before doing that, the difference between "odd" and "even" models is addressed, since this is of relevance for our experimentally observed difference between dendrons and dendrimers.

2.5. "Odd–Even" Effect: Importance of Saturation in Multivalent Catalysts. The "odd" and "even" models are analogous multivalent systems in the sense that both contain identical catalytic sites (composed of two units) with identical Michaelis–Menten parameters k_{di} and K_{di}. However, the simulations and the "retro"-fitting using the Michaelis–Menten equation show some peculiar differences between the two series.

Importantly, although the "odd" models have identical catalytic sites compared to the "even" models, the resulting $k_{cat,unit}$ values are lower (Figure 7a) and are not constant. The reason is that complete saturation of all catalytic units is not possible for the "odd" models since the catalytic site is composed of two units. The abundance of the single catalytic unit that does not contribute to catalysis at saturation makes the system appear less active. Obviously, this becomes less important when the valency increases and, in fact, $k_{cat,unit}$ for the "odd" models asymptotically reaches the level of the "even" models. The observed difference in $k_{cat,unit}$ between "odd" and "even" models is important, since it illustrates that the $k_{cat,unit}$ value depends on the extent to which a multivalent system can be saturated and not necessarily reflects the efficiency of the catalytic site. This is of practical relevance in case the saturation behavior of two structurally related, but different, multivalent series is compared (for instance, dendrons d_2-d_{16} and dendrimers D_4-D_{32}).

Remarkably, the K_M values show an opposite trend, being much lower for "odd" models (Figure 6b). This indicates an

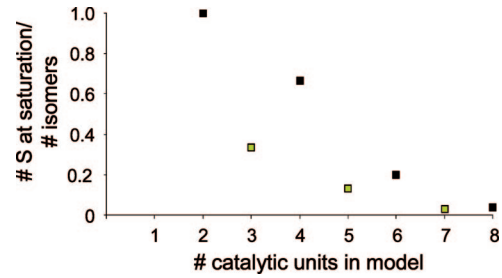

Figure 11. Plot of the number of substrate molecules bound at saturation divided by the number of isomers for the saturated complex against the dendrimer valency.

'apparent' stronger binding of substrates to "odd" models compared to "even" ones. The origin of the difference between "odd" and "even" models can also be traced back to statistics. As example, consider "odd" model E_3 which at saturation has one substrate molecule bound (E_3S_{d1}). The complex E_3S_{d1} can be formed in three different ways, depending which catalytic units are involved in substrate binding. On the other hand, "even" model E_4 has two substrate molecules bound at saturation (E_4S_{d2}). However, also for complex E_4S_{d2} only three isomeric forms are possible, since binding of the first substrate molecule defines the position of the second substrate molecule. As a consequence, "retro"-fitting of the saturation profiles using the Michaelis–Menten equation results in a lower "apparent" K_M value (indicating stronger binding) for "odd" model E_3 compared to "even" model E_4. In fact, a plot of the number of substrate molecules bound under saturation divided by the number of possible isomers for the saturated complex against the number of catalytic units (Figure 11) gives a trend that nicely corresponds to the simulated behavior for K_M (Figure 6b). Based on this theoretical analysis, it appears that an experimental observation of such behavior for K_M between two series of analogous multivalent catalysts is indicative of a different level of saturation for the two series. As will be discussed next, the series of dendrons d_2-d_{16} and dendrimers D_4-D_{32} represent such a case.

2.6. Interpretation of the Experimental Data. After this theoretical analysis, the question is whether the conclusions are also valid to explain experimental observations. From the theoretical analysis it is clear that the critical parameters are the first-order rate constant per catalytic unit ($k_{cat,unit}$ obtained by dividing $k_{cat,den}$ by the number of catalytic sites) and the dissociation constant (K_M). These values are plotted in Figure 12a and b for dendrons d_2-d_{16} and dendrimers D_4-D_{32} as a function of the number of catalytic units present. Figure 12c reports the resulting second-order rate constant ($k_{cat,unit}/K_M$).

As a general observation, it becomes immediately clear that the series of dendrons and dendrimers have quite different

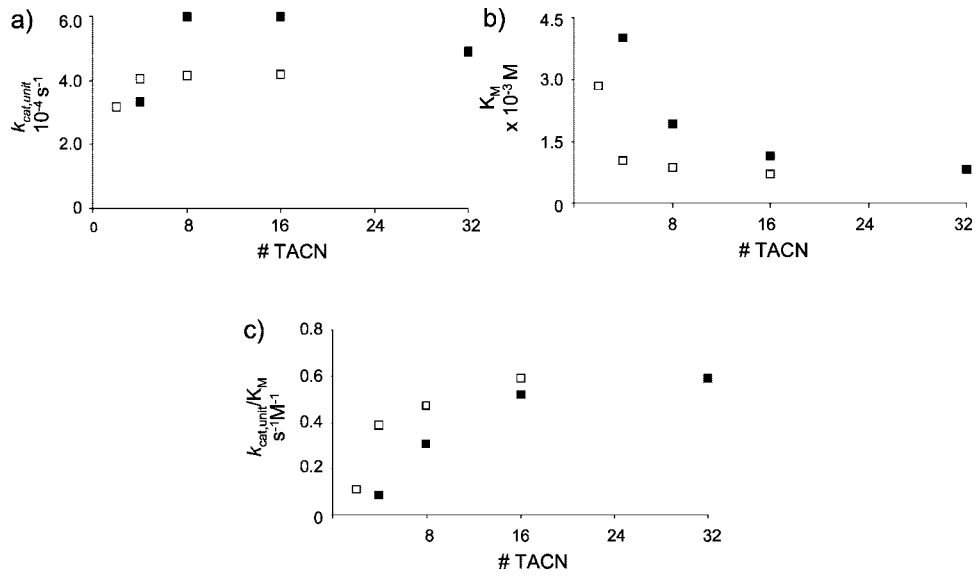

Figure 12. Plots of (a) $k_{cat,unit}$, (b) K_M, and (c) $k_{cat,unit}/K_M$ as a function of the number of catalytic units (TACN) present in dendrons d_2-d_{16} (□) and dendrimers D_4-D_{32} (■).

characteristics, in terms of both $k_{cat,unit}$ and K_M, although both classes display a similar trend upon increasing the valency. The origin of the difference between dendrons and dendrimers will be discussed later. First, the general tendencies of $k_{cat,unit}$ and K_M will be discussed. Considering $k_{cat,unit}$, the most important observation is that for the dendron series $k_{cat,unit}$ increases (slightly) from d_2 to d_4, after which it remains constant up to d_{16}. For the dendrimer series a jump in activity is observed from D_4 to D_8, but after that also in this series the activity per catalytic site remains constant (except for D_{32}, which will be discussed later). Apparently, upon reaching d_4 for the dendron series and D_8 for the dendrimer series, the maximum dendritic effect in terms of creating catalytic sites is reached. Any additional increase in valency is of *no relevance for the activity of the individual catalytic site*. The observed increase in the "overall" rate constant $k_{cat,den}$ is entirely numerical. In fact, although the highest "overall" rate constant is observed for dendrimer D_{32} ($k_{cat,den} = 15.6 \times 10^3$ s^{-1}), analysis of $k_{cat,unit}$ shows that the catalytic units in this dendrimer are in fact performing worse than its smaller analogues D_8 and D_{16}.

Whereas the catalytic efficiency per unit is largely independent of the dendron or dendrimer generation, the K_M value for both dendrons and dendrimers continuously decreases upon increasing the generation. In analogy with other systems, this would normally be ascribed to the formation of a microenvironment within the dendrimer which causes an enhanced substrate binding. However, considering the fact that this trend is identical to that predicted by the theoretical model based on statistical possibilities of forming catalytic sites (Figure 6b), a chemical explanation is not necessary at all. Increasing the dendrimer generation simply increases the apparent concentration of catalytic sites which consequently automatically results in an apparent stronger binding.

A plot of $k_{cat,unit}/K_M$ versus the number of catalytic units gives an idea about the efficiency of these dendrimers in generating catalytic sites. As illustrated in the theoretical analysis, a maximum efficiency upon increasing dendrimer generation gives a linear relation between $k_{cat,unit}/K_M$ and the number of catalytic units (Figure 7b). For dendrons d_2-d_{16} and dendrimers D_4-D_{32} the increase in the second-order rate constant $k_{cat,unit}/K_M$ is significantly lower and, in fact, seems to level off at high generations. This trend is identical to that simulated for a system in which the maximum number of binding sites is not generated upon the addition of a new dendrimer generation (Figure 10b). The observation that the parameter $k_{cat,unit}/K_M$ was only slightly affected by even large changes in the statistical coefficients indicates that from this perspective the multivalent catalysts reported here, although very potent, behave rather poorly.[57] Apparently, upon the addition of a new generation the number of potential binding sites increases relatively little, especially for the higher generations. This can be rationalized considering the backbone structure of these structures, which are composed of lysine residues. The asymmetric nature of this branching unit results in a dispersion of the TACN-ligands in the dendrons with some of them located at the periphery and others closer to the core. This spatial difference becomes larger for each generation added.

What remains is a discussion on the difference between the dendrons and dendrimers. Both classes of multivalent catalysts display a similar trend (constant $k_{cat,unit}$ and decreasing K_M), but the dendrimer series is characterized by a higher $k_{cat,unit}$ value (higher activity), but also a higher K_M ("apparent" weaker binding). Generally, a higher $k_{cat,unit}$ would be ascribed to a catalytic site with improved properties. However, considering the structural similarities between dendrons and dendrimers this does not seem very likely. The argument that dimerization induces changes in the structure and, in so doing, optimizes the catalytic site does not hold, since in that case also *within* the dendron and dendrimer series $k_{cat,unit}$ should increase. This is clearly not the case. Experimental evidence for the fact that the catalytic sites in dendron d_{16} and dendrimer D_{16} are identical was obtained by performing a "reversed" Michaelis–Menten kinetics, i.e., increasing the amount of catalyst at a constant substrate concentration. In such a case, at saturation a maximum of one substrate molecule is bound to the multivalent catalyst and thus provides a tool to probe a single catalytic site.[50] The

(57) A linear relation between $1/K_M$ and valency has been observed experimentally by Reymond *et al.*[40] for peptide-based dendrimer catalysts. The impressive results of these multivalent catalysts in terms of generating catalytic sites is probably caused by the presence of catalytic histidine units in each generation, rather than only in the periphery of the dendrimer.

initial rate v_{init} was measured at a constant HPNPP concentration of 2×10^{-5} M and a concentration of TACN ranging from 1×10^{-5} to 4×10^{-4} M. Fitting of the obtained saturation curves to the Michaelis–Menten equation gave k_{cat} values of 8.6×10^{-5} s^{-1} and 8.4×10^{-5} s^{-1} for dendron d_{16} and dendrimer D_{16}, respectively, and K_M values of 1.28×10^{-4} and 1.38×10^{-4} M, respectively. The almost identical values for k_{cat} indicate that the catalytic sites in dendron d_{16} and dendrimer D_{16} are equally active. Assuming an identical catalytic activity for all catalytic sites present in the multivalent structures, dividing the rate constant $k_{cat,unit}$ obtained under substrate saturation conditions by these newly obtained values yields the number of catalytic sites in each structure.[50,58] Interestingly, these calculations show that dendron d_{16} contains only 5 catalytic sites ($4.17 \times 10^{-4}/8.6 \times 10^{-5}$) against 7 ($6.0 \times 10^{-4}/8.4 \times 10^{-5}$) for dendrimer D_{16}. It is worth noticing that both structures can form a maximum of 8 catalytic sites composed of two TACN−Zn^{II} complexes. Therefore, based on the theoretical analysis, we postulate that the difference between $k_{cat,unit}$ values of the dendrons and the dendrimers is caused by a different degree of saturation. At saturation the dendrimer complex D_xS_m has a higher stoichiometry than the corresponding dendron complex d_xS_n ($m > n$, with x as the number of catalytic units). Upon dimerization, catalytic sites are generated which are not present within the dendron. However, the efficiency of creating these additional sites strongly depends on the dendron generation. Dimerization of dendron d_2 to give dendrimer D_4 has only a small effect on $k_{cat,unit}$ (and K_M) which must be related to the small size of this dendron compared to the GlyCys spacer. Upon dimerization the two parts do not sense each other. For larger dendrimers "contact" between the two halves is established resulting in additional catalytic sites (and thus a higher $k_{cat,unit}$). On the other hand, this jump in activity is not observed upon dimerization of dendron d_{16} to give D_{32}. Both catalysts have nearly identical values for $k_{cat,unit}$ (Table 1), which indicates that the newly created sites are no longer accessible for substrate molecules. For dendrimer D_{32}, steric crowding limits access of substrate molecules to the catalytic sites buried inside the dendrimer. The lower degree of saturation also explains why, in terms of catalytic activity per unit ($k_{cat,unit}$), dendrimer D_{32} behaves worse than its smaller analogues D_8 and D_{16}.

Intuitively, one would argue that an increase in the number of catalytic sites would, for statistical reasons, have to result also in a lower K_M (stronger binding), but the analysis of the "odd/even" models indicates that such an argumentation is not correct when the saturation stoichiometry is different. In fact, the striking resemblance between the experimental data for the K_M values of dendrons and dendrimers (Figure 12b) and the simulated values for the "odd/even" models (Figure 6b) is in strong support of our explanation that the difference between dendrons and dendrimers is due to a different level of saturation.

3. Conclusions

We have presented a series of multivalent dendritic structures that show very high catalytic activity in the cleavage of HPNPP, an RNA model compound. The observation that the activity was strongly related to the valency of the structures and the fact that we had previously observed similar behavior in related multivalent structures prompted us to develop a theoretical model in order to understand the origin of the dendritic effect. Interpretation of our own experimental data in view of the model analysis showed that these multivalent catalysts are far from being exceptional, despite the fact that their catalytic performances at first appear outstanding in terms of rate acceleration $k_{cat,den}/k_{uncat}$ and second-order rate constant $k_{cat,den}/K_M$. The maximum $k_{cat,unit}$ values are already reached at relatively low generations and drop again for the structure with the highest valency (Figure 12a). Additionally, the value of ($k_{cat,unit}/K_M$) grows significantly less than linear as a function of valency (Figure 12c), indicating that the formation of accessible catalytic sites upon valency is not optimal.

Generally, the efficiency of multivalent catalysts is described using the Michaelis–Menten parameters $k_{cat,den}$ and K_M. However, our analysis suggests that these "averaged" parameters by themselves are flawed indicators of catalytic efficiency, the first one being numerically inflated, the second one being compiled of all separate binding events that occur. The question is how to use these parameters for the evaluation of multivalent catalysts. It appears that the potency of a multivalent catalyst depends largely on two issues: first, the extent to which the multivalent catalyst can be saturated or, in other words, the number of catalytic units that are effectively participating in catalysis under saturation conditions; second, the efficiency of the multivalent system in increasing the apparent concentration of catalytic sites composed of two (or more) catalytic units. This has the following consequences for the experimental parameters $k_{cat,unit}$ and K_M.

The value of $k_{cat,unit}$ in a given system appears to be independent of its valency. A positive dendritic effect here implies that $k_{cat,unit}$ increases as a function of valency.[59] This might result from the formation of a catalytic site composed of two catalytic units at low valencies or also three units (at higher valencies) which may lead toward mechanistically different pathways. An increase in $k_{cat,unit}$ may also have a "chemical" origin, for instance, a change in local pH or a conformational change. Alternatively, a decrease in $k_{cat,unit}$ indicates that the system loses efficiency because the steric size inhibits access of the substrate to some catalytic sites, resulting in a decreased level of saturation.

As for the value of K_M, the observation of a linear correlation between $1/K_M$ and valency by itself is not an indication of a positive dendritic effect. However, it is clear that a system displaying such linear behavior is extremely efficient in creating catalytic sites.[40] Positive dendritic effects, for instance, due to the formation of a hydrophobic microenvironment, are evident only in case a plot of $1/K_M$ against valency increases more than linear. On the other hand, for a less efficient multivalent catalyst the value of $1/K_M$ will level off at higher valencies.

In summary, this study of multivalent enzyme-like catalysts sheds new light on the origin of the dendritic effect displayed by these systems. The analysis of the model clearly shows that the dendritic effect is an intrinsic consequence of clustering catalytic units in a multivalent structure in case the catalytic pathway involves two or more catalytic units. Obviously, this does not exclude, as frequently reported, that the dendritic effect is additionally induced by alterations of chemical parameters, but this has to be specifically proven. Although here the attention was focused on dendrimer catalysts it is clear that the discussion is also valid for other multivalent systems, ranging from small, tripodal catalysts to self-assembled monolayers on Au nano-

(58) Hollfelder, F.; Kirby, A. J.; Tawfik, D. S. *J. Am. Chem. Soc.* **1997**, *119*, 9578–9579.

(59) Francavilla, C.; Drake, M. D.; Bright, F. V.; Detty, M. R. *J. Am. Chem. Soc.* **2001**, *123*, 57–67.

particles, polymers, and self-assembled structures. Our analysis provides a better understanding of the origin of the dendritic effect and indicates that a careful interpretation of the experimental data is of importance for assessing the efficiency of multivalent catalysts.

4. Experimental Section

Solvents and reagents were purchased from commercial sources and used without further purification. The diBoc-TACN acetic acid (2-(1-(4,7-bis(*tert*-butyloxycarbonyl)-1,4,7-triazacyclononane)-acetic acid) was synthetized using a previously reported procedure.[26] HPNPP (2-hydroxypropyl *p*-nitrophenyl phosphate) was synthetized according to a literature procedure.[60] Dendrons were synthesized using standard peptide synthesis protocols (see below) following the synthetic route depicted in Scheme 1.

4.1. Fmoc Removal. The resin was treated with a solution of 20% of piperidine in DMF for 10 min, filtered, and washed (2× each) with DMF and CH_2Cl_2. The procedure was repeated.

4.2. Coupling of the First Amino Acid on Resin. The resin was treated to remove the Fmoc group. Fmoc-Gly-OH (3 equiv) was dissolved in DMF/CH_2Cl_2 1:1, and then HOBt (1-hydroxybenzotriazole, 4 equiv), EDC (*N*-(3-dimethylaminopropyl)-*N*′-ethylcarbodiimide, 4 equiv), and DIPEA (*N*,*N*-diisopropylethylamine, 20 equiv) were added. After 10 min the solution was added to the resin, and the mixture was stirred for 2.5 h. The resin was filtered and washed (3× each) with DMF and CH_2Cl_2. The procedure was repeated, after which quantitative coupling was checked with the Kaiser test.

4.3. Coupling of the Amino Acids on the Free Amines (General Procedure). The amino acid (3 equiv relative to the free NH_2) was dissolved in a 1:1 mixture of DMF/CH_2Cl_2, after which HBTU (*O*-(benzotriazol-1-yl)-*N*,*N*,*N*′,*N*′-tetramethyluronium hexafluorophosphate, 4 equiv), HOBt (4 equiv), and *N*-methylmorpholine (20 equiv) were added. After 10 min the solution was added to the resin, and the mixture was stirred for 2 h 30 min. The resin was filtered and washed (3× each) with DMF and CH_2Cl_2. The procedure was repeated until the coupling was complete (Kaiser test).

4.4. Cleavage. The resin was treated with the cleavage mixture (CH_2Cl_2, triisoproylsilane, trifluoroacetic acid 1/1/8 plus one drop of water) for 1.5 h. The resin was filtered, and the solution was evaporated under vacuum. The peptide was precipitated from methanol/diethyl ether and purified using RP HPLC (Agilent Zorbax, C18, 300 Å (A: H_2O + 0.1% TFA, B: CH_3CN + 0.1% TFA; gradient: 5% B (0–5 min), 5–50% B (5–20 min). A stock solution of the dendrons was prepared dissolving the solids in a 1:1 mixture of H_2O/CH_3CN.

4.5. Quantification of Thiol Groups. The concentration of the dendron in the stock solution was determined by the quantification of the free thiols using the Ellmann's reagent (DTNB, 5,5′-dithiobis(2-nitrobezoic acid)). 40 μL of stock solution of DTNB (2 mM in sodium acetate 0,05 M) and 8 μL of stock solution of dendron were added to 400 μL of a 0.1 M solution of phosphate buffer pH 7.0. The concentration of free thiol was determined measuring the absorbance at 412 nm (ϵ_{412} = 13 470 $L \cdot mol^{-1} \cdot cm^{-1}$ based on a calibration curve obtained from Cys).

4.6. Blocking of Free Thiol in Dendrons. 200 μL of stock solution of dendron were added to 800 μL of a 1:1 mixture of a 0.1 M phosphate buffer at pH 7.0 and acetonitrile, after which 1.5 equiv of *N*-ethylmaleimide (from a 0.05 M solution in methanol) were added. The completion of the reaction was confirmed by a negative Ellman's test.

4.7. Dimerization of Dendrons. 400 μL of a NaOH solution in water at pH 10 and 400 μL of acetonitrile were added to 200 μL of the stock solution of dendron; the solution was stirred by bubbling air through the reaction mixture until the completion of disulfide formation was confirmed by Ellman's test (absence of thiols).

4.8. Kinetic Measurements. Kinetics were measured at 40 °C in aqueous solution containing 30% of acetonitrile, buffered at pH 7.5 with HEPES 0.01 M. Reaction mixtures were prepared by adding in order the solution of dendron or dendrimer, a solution of $Zn(NO_3)_2$, and a solution of HPNPP in water. The experiments were performed in 96-well plates (Greiner) in a volume of 250 μL; the cleavage of the phosphodiester was monitored by measuring the absorbance of *p*-nitrophenolate at 405 nm; the plates were sealed with a cover to prevent evaporation. Initial velocities were calculated by a linear fitting of the initial part of the kinetics (conversion <10%).

4.9. Dendron d_2. HPLC (Agilent Zorbax, C18, 300 Å (A: H_2O + 0.1% TFA, B: CH_3CN + 0.1% TFA; gradient: 5% B (0–5 min), 5–50% B (5–20min)): 13.8 min (100%). MS (ESI-(+), (H_2O + 0.1% HCOOH)/(CH_3CN + 0.1% HCOOH) = 1:1): *m*/*z* 645.0 (calcd $(M + H)^+$: 644.4).

4.10. Dendron d_4. HPLC (Agilent Zorbax, C18, 300 Å (A: H_2O + 0.1% TFA, B: CH_3CN + 0.1% TFA; gradient: 5% B (0–5 min), 5–50% B (5–20 min)): 14.8 min (100%). MS (ESI-(+), (H_2O + 0.1% HCOOH)/(CH_3CN+0.1% HCOOH) = 1:1): *m*/*z* 1238.8 (calcd $(M + H)^+$: 1238.8), 620.0 (calcd $(M + 2H)^{2+}$: 619.9), 413.7 (calcd $(M + 3H)^{3+}$: 413.6), 310.6 (calcd $M + 4H)^{4+}$: 310.5).

4.11. Dendron d_8. HPLC (Agilent Zorbax, C18, 300 Å (A: H_2O + 0.1% TFA, B: CH_3CN + 0.1% TFA; gradient: 5% B (0–5 min), 5–50% B (5–20 min)): 16.3 min (100%). MS (MALDI-TOF Perseptive Biosystems Voyager-DE-PRO): 2430 (calcd $(M + H)^+$: 2428)).

4.12. Dendron d_{16}. HPLC (Agilent Zorbax, C18, 300 Å (A: H_2O + 0.1% TFA, B: CH_3CN + 0.1% TFA; gradient: 5% B (0–5 min), 5–50% B (5–20 min)): 17.0 min (100%). MS (MALDI-TOF Perseptive Biosystems Voyager-DE-PRO): 4800 (calcd $(M + H)^+$: 4804)).

4.13. Dendrimer D_4. HPLC (Agilent Zorbax, C18, 300 Å (A: H_2O + 0.1% TFA, B: CH_3CN + 0.1% TFA; gradient: 5% B (0–5 min), 5–50% B (5–20 min)): 13.1 min (100%). MS (ESI-(+), (H_2O + 0.1% HCOOH)/(CH_3CN + 0.1% HCOOH) = 1:1): *m*/*z* 1286.0 (calcd $(M + H)^+$: 1285.8).

4.14. Dendrimer D_8. HPLC (Agilent Zorbax, C18, 300 Å (A: H_2O + 0.1%TFA, B: CH_3CN + 0.1%TFA; gradient: 5% B (0–5 min), 5–50% B (5–20min)): 14.6 min (100%).

4.15. Dendrimer D_{16}. HPLC (Agilent Zorbax, C18, 300 Å (A: H_2O + 0.1% TFA, B: CH_3CN + 0.1%TFA; gradient: 5% B (0–5 min), 5–50% B (5–20 min)): 15.6 min (100%).

4.16. Dendrimer D_{32}. HPLC (Agilent Zorbax, C18, 300 Å (A: H_2O + 0.1% TFA, B: CH_3CN + 0.1% TFA; gradient: 5% B (0–5 min), 5–50% B (5–20 min)): 16.5 min (100%).

Acknowledgment. The authors thank the University of Padova (CPDA054893) and MIUR (PRIN2006) for financial support.

Supporting Information Available: Mathematical treatment of model E_n, implementation of the models E_2–E_8 in the simulation software,[54] saturation profile of the TACN-Zn^{II} complex, theoretical analysis for both single- and double site catalysis. This material is available free of charge via the Internet at http://pubs.acs.org.

(60) Brown, D. M.; Usher, D. A. *J. Chem. Soc.* **1965**, 6558–6564.

JA7113213